Assimilation of satellite data by 3D-Var at ECMWF

E. Andersson, J. Pailleux*, J.R. Eyre,
A.P. McNally, G.A. Kelly, P. Courtier and F. Rabier

European Centre for Medium-Range Weather Forecasts, Reading, U.K.
*Current affiliation, Météo-France, Toulouse, France

1. INTRODUCTION

The TOVS (TIROS-N Operational Vertical Sounder) instrument on the NOAA series of polar orbiting satellites measures radiances which are sensitive to the temperature and humidity of the atmosphere (Smith *et al.*, 1979). These data have traditionally been used in numerical weather prediction (NWP) in the form of temperature and humidity profiles, obtained through an inversion process known as "retrieval". The retrieved profiles are then used together with all other observations to form an analysis which after initialisation is used as the starting point for a forecast.

In this paper, we have used TOVS radiances directly, as described by Andersson *et al.* (1994), in a three-dimensional variational analysis scheme (3D-Var) (Courtier *et al.*, 1993). In 3D-Var, horizontal as well as vertical consistency in the use of the radiances is ensured. The TOVS data are used together with all other data. Mass, wind and humidity are analysed simultaneously under certain balance constraints which control the level of gravity waves in the analysis. The scheme thus combines retrieval, analysis and initialisation in one step.

The advantage of variational schemes, in the context of TOVS retrieval/analysis, is in the use of more accurate background information (a six-hour forecast) and an appropriate forecast error covariance as a constraint. For a one-dimensional scheme, like the operational 1D-Var scheme (Eyre *et al.*, 1993), this introduces a correlation between the observation error and the background error, which may cause problems when the same six-hour forecast is used again as the background for the subsequent analysis (as discussed by Eyre *et al.*). The problem disappears in a three or four-dimensional variational scheme where retrieval and analysis are combined, and hence the background is used only once. Radiances are then used directly together with all other observations and the background field.

In this paper we show that 3D-Var with radiances works well in data assimilation experiments. The quality of the forecasts clearly improves on average over a 14-day period, compared to the operational

OI scheme. The results are strongly dependent on the specification of vertical correlations of the forecast error for temperature. In agreement with Phillips (1986), we found that a non-separable formulation of forecast error is necessary in order to have the correct structures for wind as well as temperature.

The variational method is described briefly in section 2. In section 3 we show results from the validation of the system when applied to a simplified retrieval/analysis problem with an analytical solution. Section 4 describes the non-separable formulation of forecast error correlations. We present results from two weeks of data assimilation with 3D-Var (section 5) and compare with an OI analysis which had used profiles retrieved by the operational one-dimensional variational method. We conclude that the non-separable formulation of 3D-Var generally performs well.

2. METHOD

2.1 Variational formulation

We follow the general variational approach to the assimilation of data into an NWP system (Lorenc, 1986; Talagrand, 1988) by minimizing the cost-function $J(x)$ with respect to the atmospheric state x, where $J(x)$ measures the degree of mis-fit to the observations, to the background information and to the slow manifold. If the errors involved have Gaussian distributions, then the optimal penalty function is a sum of quadratic terms:

$$\begin{aligned} J(x) &= J_o + J_b \quad (+ J_c) \\ J_o &= [y - H(x)]^T O^{-1} [y - H(x)] \\ J_b &= (x - x_b)^T B^{-1} (x - x_b) \end{aligned} \tag{1}$$

where x_b is the background with estimated error covariance B, y represents the observations with estimated error covariance O, and H is the observation operator (or "forward" operator) which computes model equivalents of the observed quantities at the observation points. The matrix O should in addition to the observation error also include the representativeness error, i.e. the error in the forward operator. J_c is an optional term in the cost function measuring the distance to the slow manifold, i.e. the amount of gravity waves in the analysis.

Eq.1 applies to a wide range of problems. It has the same form in one as well as three and four-dimensional applications. In the case of TOVS radiances, H specifically represents the radiative transfer model which calculates radiances from the state vector of the forecast model. In 4D-Var, H includes a model integration from the time of the background to the time of the observation (see Thépaut *et al.*, 1993). 3D-Var is thus, in theory as well as in practice, equivalent to a 4D-Var without

model integration.

The solution in the linear case, is given by:

$$x_a - x_b = BH'^T (H'BH'^T + O)^{-1} [y - H(x_b)] \quad (2)$$

where $x_a - x_b$ represents the analysis increment (analysis minus background). H' contains the partial derivatives of $H(x)$. In the nonlinear case, the solution can be found through e.g. Newtonian iteration (Rodgers, 1976; Eyre, 1989) or through the adjoint technique as described by Le Dimet and Talagrand (1986) and applied to the retrieval problem by Thépaut and Moll (1990). Details particular to the IFS/Arpège implementation of the adjoint technique have been documented in Pailleux *et al.* (1991) and Courtier *et al.* (1993).

At the minimum, the second derivative of the cost function, $J''(x)$, represents the inverse of the analysis error covariance, A. Omitting terms involving the gradient of $H'(x)$ we have:

$$J''(x) = A^{-1} = B^{-1} + H'^T O^{-1} H' \quad (3)$$

2.2 Simultaneous analysis of TOVS and other observations

Use H and O for the TOVS observation operator and the observation error covariance, respectively. Similarly, use G and Q for any other observations. G could represent the vertical integration of the hydrostatic equation to form model equivalents of geopotential height measurements, for example.

The expression for the analysis error (A) is (from Eq.3):

$$A^{-1} = B^{-1} + H'^T O^{-1} H' + G'^T Q^{-1} G' \quad (4)$$

The equivalent analysis can be achieved in two steps. First a "retrieval" step:

$$A_1^{-1} = B^{-1} + H'^T O^{-1} H' \quad (5)$$

Followed by an "analysis" step:

$$A_2^{-1} = A_1^{-1} + G'^T Q^{-1} G' \quad (6)$$

We note that $A_2 = A$, provided the appropriate retrieval error covariance matrix (A_1) is used in the analysis step. Ignoring the horizontal aspects, this would involve passing with every TOVS point its vertical retrieval error covariance matrix. Although this is possible in theory, practical considerations (huge data volumes) lead to simplifications of the error statistics passed from the retrieval to the analysis step. In the ECMWF implementation of 1D-Var followed by OI, for example, a set of three pre-computed vertical covariance matrices is used, one for each retrieval type: clear, partly cloudy and

cloudy. In 3D-Var, on the other hand, O is specified in terms of radiances and the appropriate observation error covariance in terms of the control variable, $H'^T O^{-1} H'$, appears implicitly, complete with the correct spatial variation.

The "retrieval" in any one point in a three-dimensional "retrieval/analysis" depends on the radiances in the neighbouring points. It can e.g. draw closely to a batch of radiances which support each other. In the hypothetical case of several coincident and identical radiance data, 3D-Var will produce as solution the temperature profile which best fits the radiances. A separate retrieval, however, will separately for each observation give a temperature profile which is a compromise between the observed radiances and the background, independently of the other coincident data. An analysis following the retrieval, cannot draw closer to the data than the retrieval did.

The arguments so far have assumed that the observation operators are linear. In the nonlinear case, there are additional effects of H' and G' changing with x, during the iterative minimisation process. Analysis changes in humidity, for example, introduced by conventional observations or by TOVS data themselves would lead to a modified H, which would affect the TOVS retrievals in the vicinity.

In principle, not only does the retrieval/analysis become more accurate during the minimisation, but also its error estimate becomes more accurate. This will produce a more nearly optimal combination of the information from TOVS, from other data types and from the background, than is possible in the traditional approach with separate retrieval and analysis steps.

The sequence of operators needed to go from spectral fields of temperature, specific humidity and surface pressure to equivalents of the TOVS observed radiances, and the subsequent calculation of the TOVS observation cost function, have been described by Andersson *et al.* (1994) and in the proceedings of the ECMWF 1992 workshop on variational assimilation.

3. AN EXAMPLE WITH A SIMPLE ANALYTICAL SOLUTION

Consider the univariate temperature analysis of *one* radiance datum at *one* location. Assume that temperature forecast errors are constant in the vertical. With the linear approximation the temperature analysis increment $(T_a - T_b)$, is given by (from Eq.2):

$$T_a - T_b = BH'^T (H'BH'^T + \sigma_o^2)^{-1} [y - H(x)] \qquad (7)$$

where, with the above simplifications:

H' is $\partial H/\partial T_i$, and T_i is temperature at model level i

$\boldsymbol{B}$ is the temperature vertical covariance matrix of background error

σ_o^2 is the observation error variance of the channel in question

$\boldsymbol{H'BH'^T}$ is the radiance equivalent of the forecast error variance, for that channel

For the vertical distribution of the analysis increment (ignoring the amplitude), Eq.7 simplifies to:

$$T_a - T_b \propto BH'^T \tag{8}$$

The matrix $\boldsymbol{H'}$ represents the sensitivity of a given TOVS channel to the temperature at discrete model levels. The matrix $\boldsymbol{B}$ describes how the observation increment is spread in the vertical. In the first validation experiment we simplify further and assume a diagonal $\boldsymbol{B}$. This de-couples the analysis in the vertical, and we obtain a two-dimensional analysis. Hence, the analysis increment at each level should be proportional to $\boldsymbol{H'}$.

3.1 Validation exercise

Carrying out a full T63 3D-Var analysis, with the above simplifications, using the channel MSU-2 only, gives the vertical profile of analysis increment given in Fig. 1b. Comparing with $\boldsymbol{H'}$ for MSU-2 as shown in Fig. 1a we see that the analysis indeed gives the expected solution.

With a non-diagonal vertical correlation matrix, the theoretical analysis increment at a given level depends on $\boldsymbol{H'}$ at all other levels, according to Eq.8. The theoretical analysis increment with the full $\boldsymbol{B}$ matrix is shown in Fig. 2a (thick line -- the thin line represents 1D-Var and will be discussed in the next section) to be compared with the actual analysis increment in Fig. 2b. The two are virtually identical, which fully validates the vertical aspects of 3D-Var.

3.2 Vertical correlation of forecast error

An important factor for the analysis of TOVS data is the specification of the vertical correlations for temperature. Since the vertical resolution of the satellite information is less than the resolution of the forecast model, the finer details in the vertical of the analysis increments are imposed by the specified prediction error covariances (Lönnberg, 1989). Lönnberg found that very noisy analysis increments could result from an improper specification of observation and forecast error statistics. Large oscillations in the temperature increments on model levels occurred in the ECMWF OI analysis when layer-mean temperatures (T_v) of thicker layers were used, i.e. T_v(1000-500) instead of T_v(1000-700) and T_v(700-500).

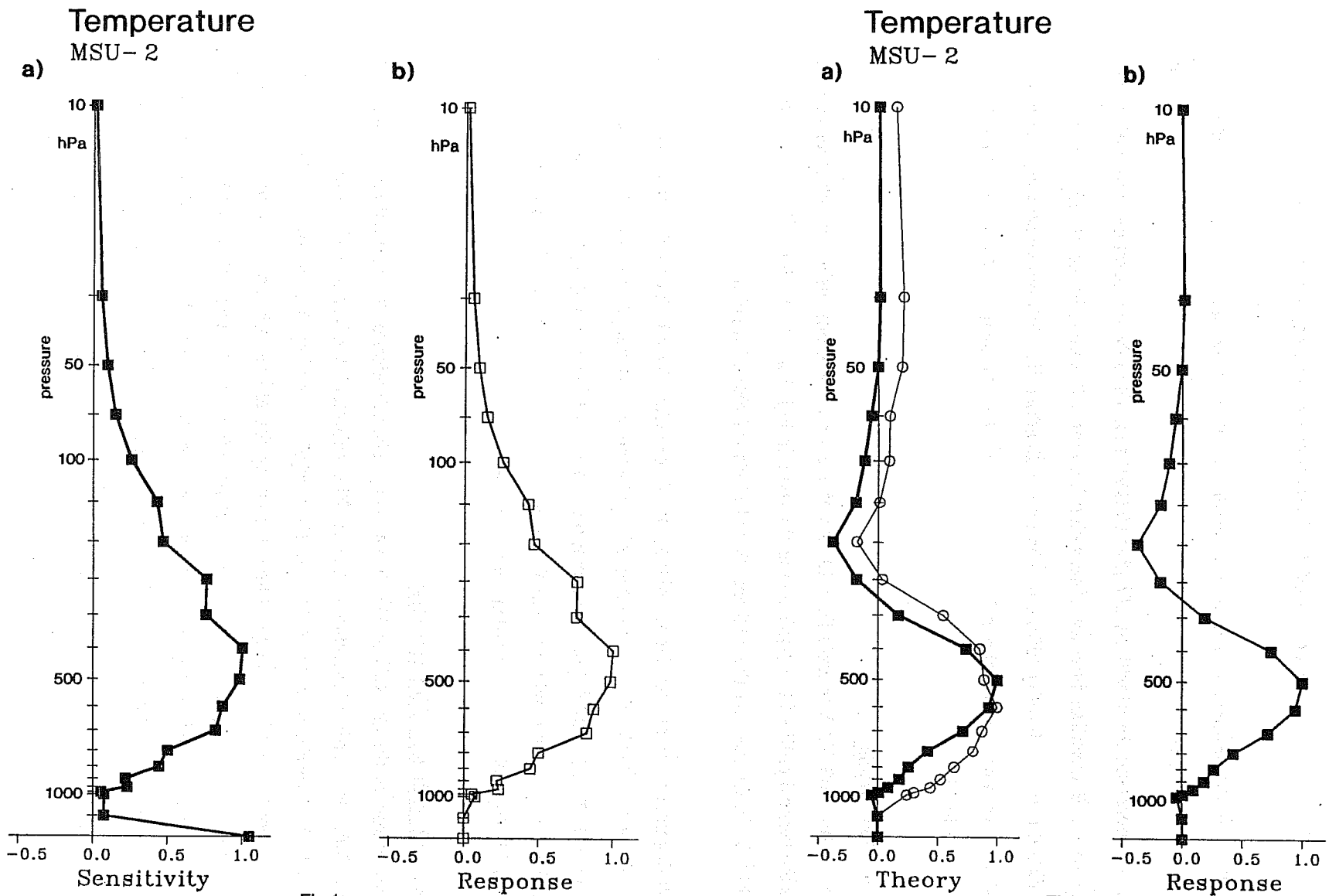

Fig.1

Fig.2

Fig.1 Shows for MSU-2: a) "Sensitivity", i.e. $H' = \partial H/\partial T_i$, the partial derivative of a TOVS channel with respect to model level temperatures and b) "Response", i.e. analysis increment, in an analysis without vertical correlations (diagonal B). The two lowest points on the curves represent T_s and T_{2m}.

Fig.2 Like Fig.1 showing a) Theoretical response (3D-Var thick, 1D-Var thin line) and b) actual response in a 3D-VAR analysis.

Similarly, oscillation in the temperature increments on model levels can occur when radiances with broad weighting functions are used directly, as in 3D-Var. This can be seen in Fig. 2a, 3b and 4b. The diagrams show the theoretical analysis increment for a given channel (when used on its own) as given by Eq.8. The thicker line refers to the vertical correlations initially used in 3D-Var (these are equal to those used by ECMWF OI over oceans at 45 North) and the thinner line is 1D-Var. The 1D-Var correlations were derived directly from temperature data (in the U.K. Meteorological Office model), Eyre *et al.* (1993), whereas the OI correlations were derived from wind and height data (Hollingsworth and Lönnberg, 1986; Lönnberg and Hollingsworth, 1986), fitted to a continuous representation for height from which temperature correlations were obtained as the first derivative in $\ln p$. The correlation between temperature at 500 hPa and all other levels is plotted as an example in Fig.5, for OI (full line) and 1D-Var (dashed).

The 1D-Var correlations are significantly broader (Fig.5) than those used by OI and give rise to a broader response in MSU-2 (Fig. 2a). For HIRS-4 (Fig. 3b) and MSU-3 (Fig. 4b), which have very broad weighting functions, we see that the sharper correlation functions of OI give rise to oscillations in the temperature increments, much like the examples of Lönnberg (1989). Oscillations do not occur with the 1D-Var vertical correlations.

3.3 Discussion

There is no good reason why 1D-Var and 3D-Var should use different forecast error statistics. A common formulation which is good for temperature as well as height and wind is needed. Rabier and McNally (1993) (called RM93 hereafter) explained that the apparent incompatibility between temperature statistics obtained directly from temperature data (as used in 1D-Var) and temperature statistics derived from height/wind statistics (as used in ECMWF OI) is due to the assumption of separability between the horizontal and vertical directions - i.e. the assumption that the correlation of the variable x between two points 1 and 2 with distance r_{12} at pressure levels p_1 and p_2 can be written as a product of two functions:

$$\text{corr}\ (x_1, x_2) = \text{function of}\ r_{12}\ \ \mathbf{X}\ \ \text{function of}\ (p_1, p_2) \qquad (9)$$

A separable formulation cannot be accurate for both wind and temperature (Phillips, 1986).

Following the ideas of Parrish and Derber (1992), RM93 used 48 minus 24 hour forecast differences for a period of one month (December 1992) at spectral resolution T106 from the operational ECMWF 31-level model, to compute covariance statistics for each total wavenumber, $n = [0, 106]$. Their set of statistics allowed the implementation of a fully non-separable formulation, which is accurate for both temperature and wind. This will be the subject of the next section.

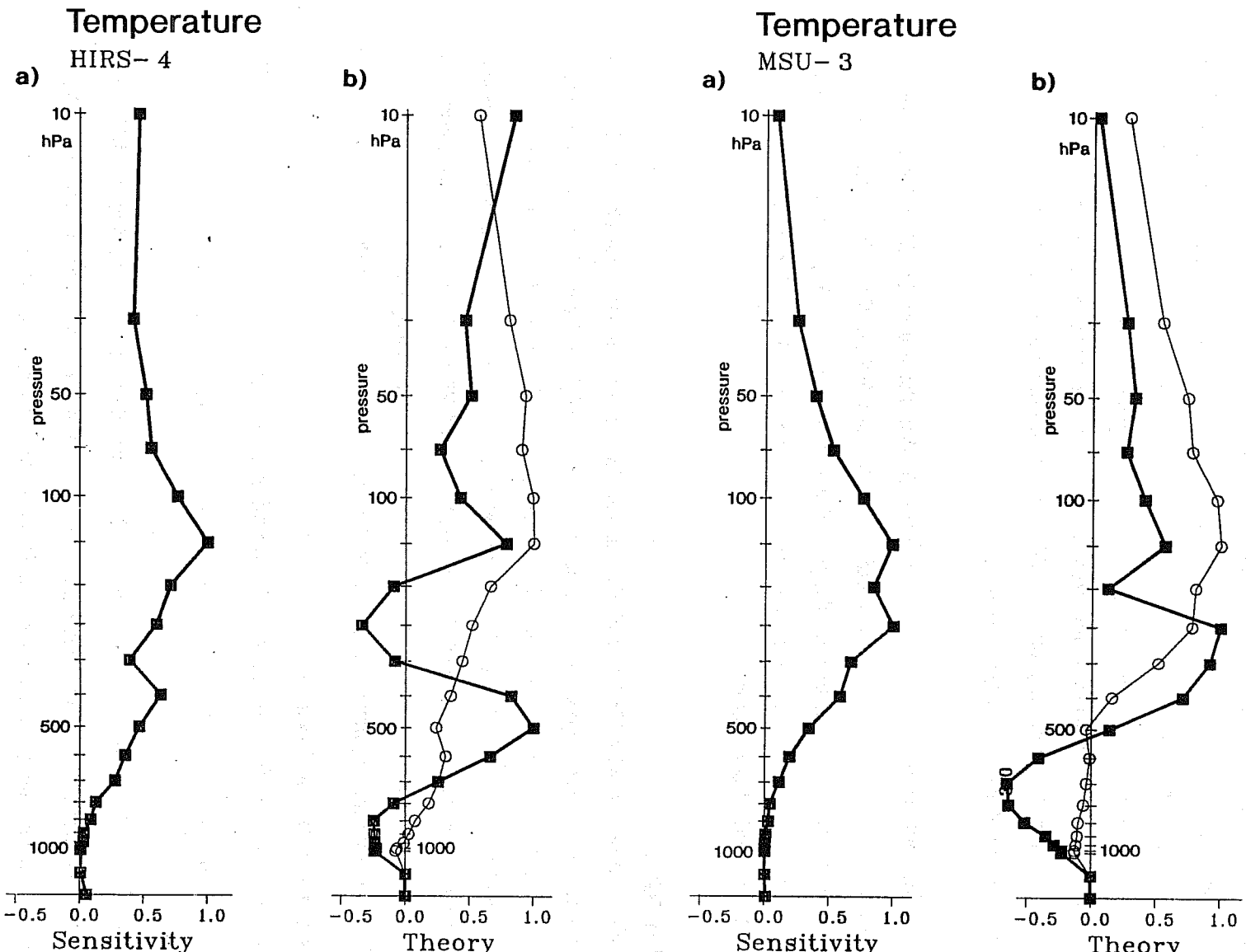

Fig.3

Fig.4

Fig.3 a) "Sensitivity" (as in Fig.1) and b) theoretical analysis increment (as in Fig.2), for HIRS-4.
Fig.4 Like Fig.3 for MSU-3.

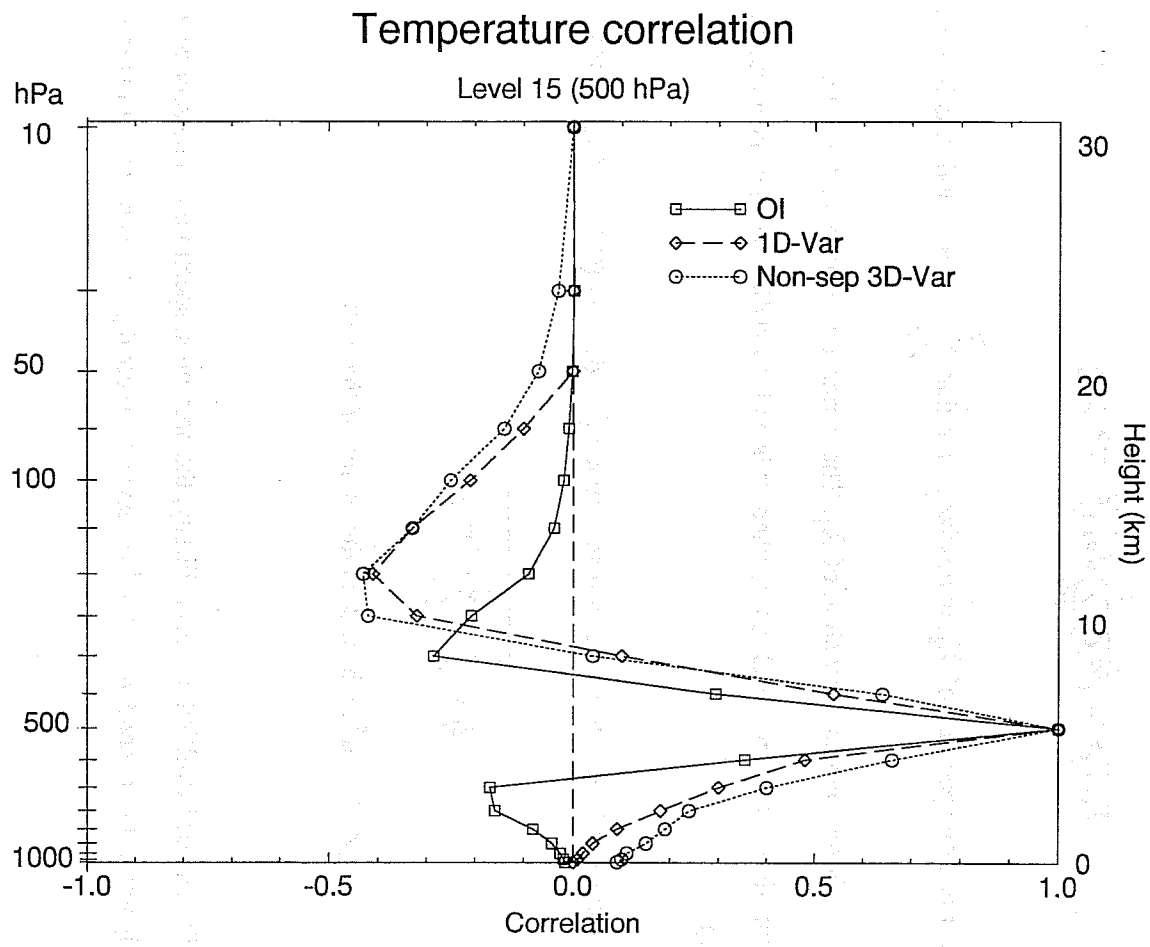

Fig.5

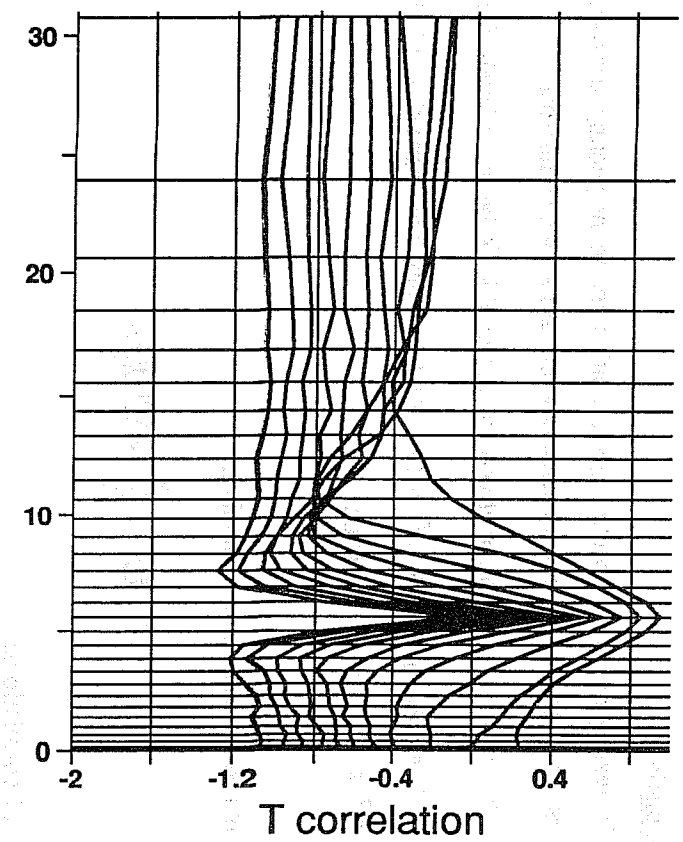

Fig.6

Fig.5 Temperature correlations for level 11 (500 hPa in a 19-level model). Those used by OI are shown in full line and those used by 1D-Var are dashed. The dotted curve represents the total vertical correlation (sum over all n) from the non-separable statistics used by 3D-Var.

Fig.6 Temperature correlations for level 18 (500 hPa, in a 31-level model) for every 10th wave-number from n=5 to 105, from RM93, artificially separated by 0.1 units along the x-direction. The numbering on the x-axis refers to n=5, which appears furthest to the right in the diagram. The horizontal lines indicate the position of model levels, L31.

4. NON-SEPARABILITY

4.1 Spectral formulation

Horizontal isotropy in real space is in spectral space equivalent to neglecting cross-covariances between wavenumbers, and neglecting the dependency on zonal wave number, m. We write $<X_i^n, X_j^n>$ to denote the covariance, of the meteorological variable X between levels i and j for total wave number n, $n = [0,N]$, where N is the spectral triangular truncation of the model. Similarly we write $[X_i^n, X_j^n]$ for the correlation.

The total covariance is a sum over all wavenumbers:

$$<X_i, X_j> = \sum_{n=0}^{N} <X_i^n, X_j^n> \tag{10}$$

or expressed in terms of correlations:

$$<X_i, X_j> = \sqrt{a_i a_j} \sum_{n=0}^{N} \sqrt{\nu_i^n \nu_j^n}\, [X_i^n, X_j^n] \tag{11}$$

where ν_i is the auto-correlation spectrum of X_i, normalized such that $\sum_{n=0}^{N} \nu_i^n = 1$ and a_i is its total amplitude, i.e. $\sqrt{a_i} = \sigma_{Xi}$ is the standard deviation of X_i. The variance spectrum ν_i translates to a horizontal correlation function $\mu(r)$ in physical space, where r is horizontal distance (see the appendix of Gauthier *et al.*, 1993).

The horizontal length scale l_i of the auto-correlation spectrum ν_i^n is defined (Daley, 1991, p110):

$$l_i = \sqrt{2 \,/\, \sum_{n=0}^{N} -\nabla^2 \nu_i^n} \tag{12}$$

with the Laplacian $\nabla^2 = -n(n+1) \,/\, a^2$, where a is the radius of the earth.

4.2 Separability

Two kinds of separability can be identified in Eq.11. Firstly, the horizontal spectrum can be separated from the vertical, i.e. ignoring the dependency of ν_i^n on level i; secondly, the vertical correlations

can be separated from the horizontal, thereby ignoring the dependency of $[X_i^n, X_j^n]$ with n. The equivalent of both kinds of separability is currently assumed in e.g. the OI scheme at ECMWF. Thus, for the covariance at each wave number:

$$<X_i^n, X_j^n> = \sqrt{a_i a_j}\ [X_i, X_j]\ v^n \tag{13}$$

and the total covariance becomes (c.f. Eq.11):

$$<X_i, X_j> = \sqrt{a_i a_j}\ [X_i, X_j] \tag{14}$$

4.3 Temperature correlations

The set of statistics obtained by RM93 comprises vertical correlations for each wavenumber as well as auto-correlation spectra for each level of the ECMWF model, for temperature, mass, wind and specific humidity - a total of several hundred thousand correlations. Rather than fitting these data with a parametric expression we found that we could use the statistics directly. An example of the variation with n of the temperature vertical correlation is shown in Fig. 6. The vertical structures are clearly broader for small n (large horizontal scales) than for large n (small horizontal scales). The total vertical correlation, calculated as a sum over all n (Eq.11) is shown as a dotted curve in Fig. 5. It shows level 11 (approximately 500 hPa) and can be compared to the curves for OI (full line) and 1D-Var (dashed). We see that the non-separable statistics give temperature correlations which agree with those obtained directly from temperature statistics (as used in 1D-Var) and not with those obtained from wind/height statistics in a separable formulation (as used in OI).

Another interesting feature is that the auto-correlation spectra for temperature have a significantly shorter length-scale (l_i, Eq.12) than for mass, Fig. 7. In the separable formulation both are the same and equal to 500 km. From the non-separable statistics we obtain length-scales for mass close to 500 km in the troposphere (Fig.7, full line), gradually increasing to 1000 km in the stratosphere, whereas the temperature length-scale (dashed) goes from 300 to 400 km.

Both these features of temperature error statistics agree with the theoretical results of Phillips (1986). It gives an indication how severely the separability assumption violates the temperature correlation structures, if the correlation model is based on mass/wind statistics. Similar problems occur in the wind and height correlation structures in a separable formulation based on temperature statistics. The operational OI system performs well because no temperature (radiance) data are used - only wind, height, thickness and humidity data. Radiance data are, as mentioned earlier, treated separately in 1D-Var using the appropriate temperature error statistics, and passed to OI in the form of thickness data.

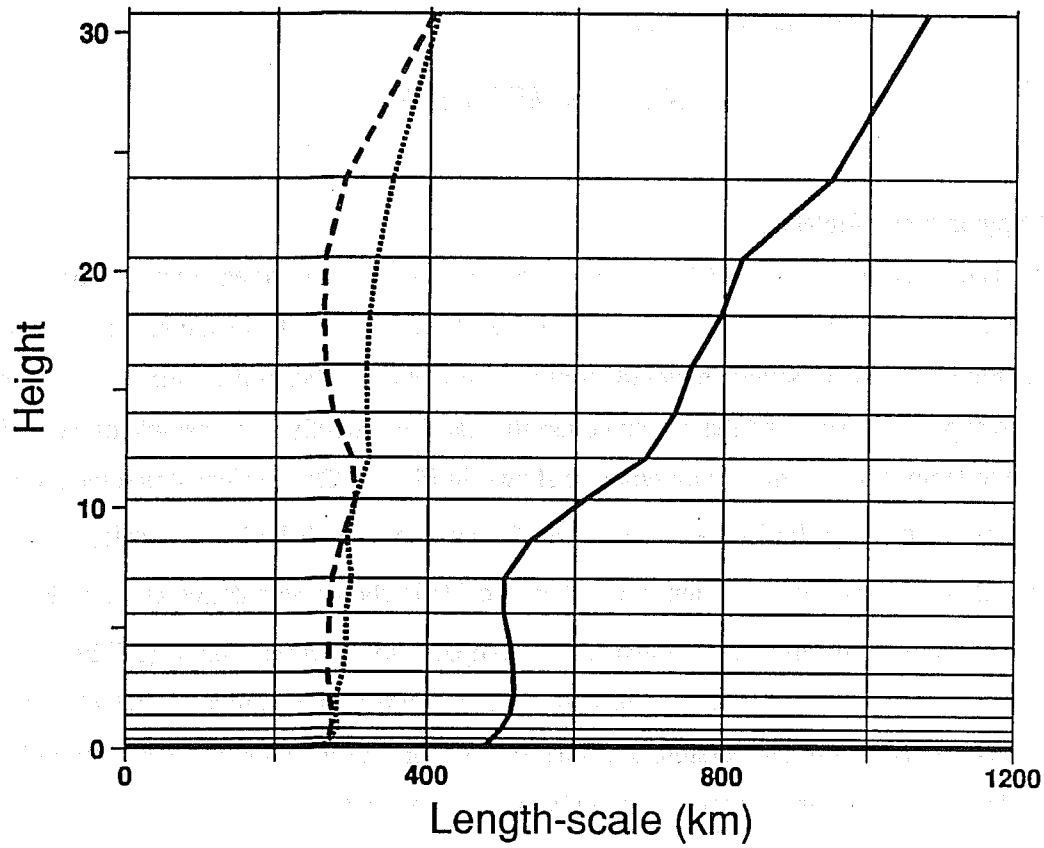

Fig.7 Horizontal length-scale for mass (full line), rotational part of wind (dashed) and temperature (dotted).

5. RESULTS OF DATA ASSIMILATION EXPERIMENTS

Result of 3D-Var in terms of single analyses were presented by Andersson *et al.* (1994). They showed generally good agreement between 3D-Var and OI analysis increments of geopotential height and wind at 500 and 50 hPa.

In this section, we compare the results in data assimilation experiments over several days. The period is 19921111-12 to 19921125-12 UT, for which we had received cloud-cleared radiances from NESDIS with nearly complete global data coverage. We have run 10-day forecast from 12 UTC at each day of the assimilations in order to use the quality of the forecast (in terms of objective scores) as a measure of the quality of the assimilations. Firstly, three 14-day 3D-Var assimilations at spectral resolution T63/L19 were performed, each with different specification of forecast error statistics, and one OI T63/L19 control. Thereafter a 14-day experiment at spectral resolution T106 was run, comparing a 3D-Var assimilation (non-separable structure functions) with OI at the same resolution. 3D-Var and OI both used the same conventional data and both used the same number of TOVS data. 3D-Var used TOVS radiances directly, whereas OI used 1D-Var retrievals everywhere on the globe, (except below 100 hPa over land).

CAA	T63/L19	Forecast error statistics from RM93. Non-separable formulation. Correct for wind and temperature.
BYN	T63/L19	The mean covariance matrix of RM93 was used, i.e. separable formulation. Correct for temperature.
BXQ	T63/L19	Forecast error covariances as in OI. Separable formulation. Correct for wind. (Stopped after 5 days.)
BXW	T63/L19	OI/1D-Var control at T63, using 1D-Var retrievals.
CDN	T106/L19	Forecast error statistics from RM93. Non-separable formulation.
CAQ	T106/L19	OI/1D-Var control at T106, using 1D-Var retrievals.

In a typical 6-hour period 3D-Var used radiances from 4,000 to 4,500 TOVS spots, in total 40,000 to 50,000 pieces of information from channels HIRS-1 to 7, 10 to 15, MSU-2 to 4 and SSU-1 and 2. In order to minimize the effect of forecast errors in surface temperature, only the seven most highly-peaking channels were used over land (HIRS-1 to 4 and 12, MSU-3 and 4, SSU-1 and 2), and from cloudy spots only the cloud-insensitive channels were used (HIRS-1 to 3, MSU 2 to 4, SSU-1 and 2).

5.2 T63 forecast results

The forecast scores (T63) of experiments CAA, BYN and BXW are presented in Fig. 8a to 8d. They

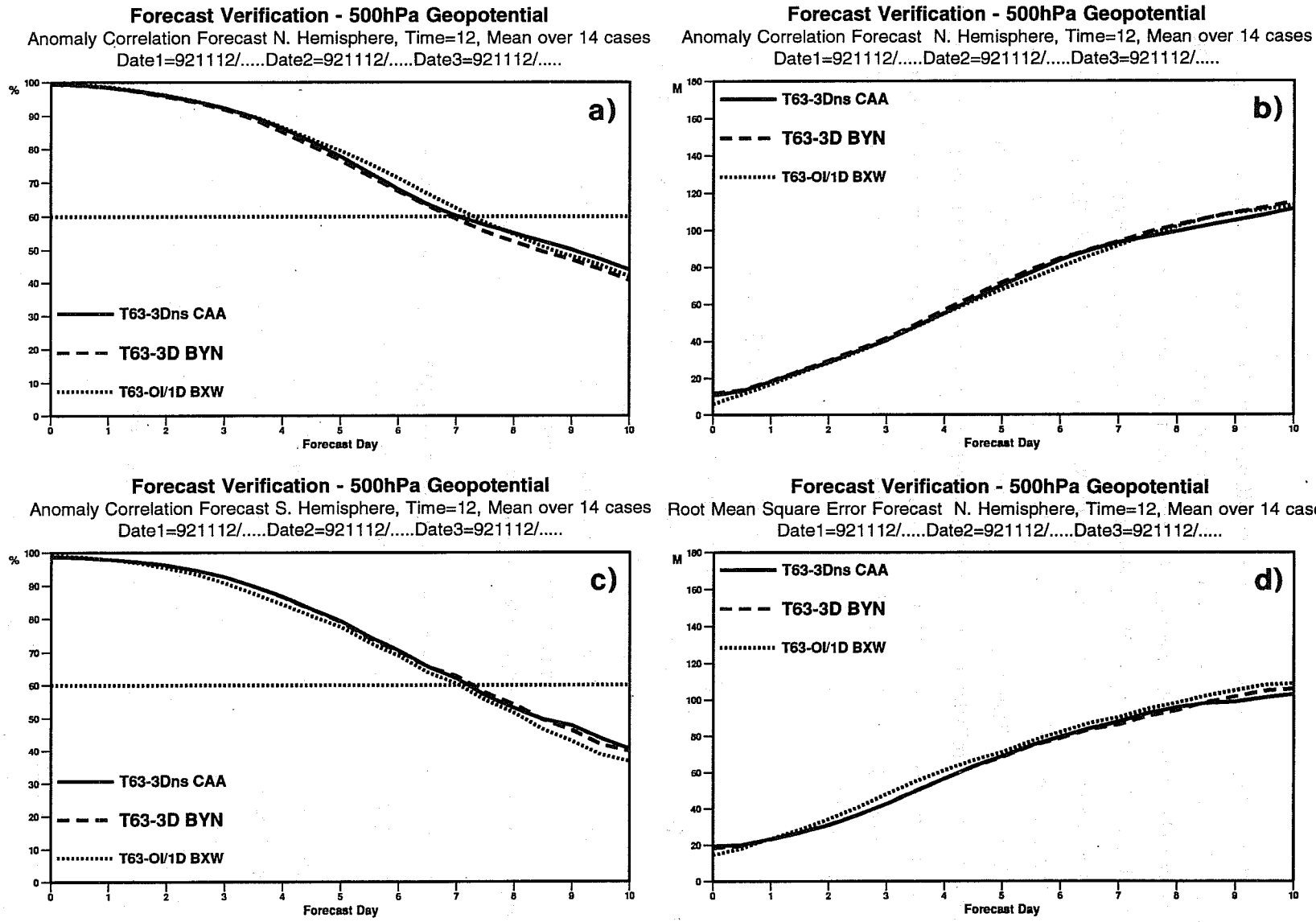

Fig.8 Anomaly correlation (left) and RMS (right) of 500 hPa forecast error of geopotential height, averaged over 14 cases, 19921112 to 19921125 12 UT. For CAA (full line), BYN (dashed) and BXW (dotted). a) and b) show Northern Hemisphere and c) and d) show Southern Hemisphere. All four are T63/L19.

are averages of 14 cases, 19921112 to 19921125-12 UT. It is quite clear that non-separability (CAA, full line) has improved the 3D-Var assimilation in the northern hemisphere, and scores are equal to the OI control (dotted line) in terms of anomaly correlations (Fig. 8a) and RMS (Fig. 8b), up to day 4. OI beats 3D-Var in the Northern Hemisphere between days 4 and 7, in this period, for these versions of 3D-Var and OI.

CAA (non-separable) performs as well as BYN (separable, temperature-based statistics) in the southern hemisphere and is clearly better than OI throughout the ten days (Fig. 8c). The improvement shows also in terms of RMS (Fig. 8d).

The experiment BXQ (which used OI-like covariances in 3D-Var, i.e. appropriate for wind) is shown separately, in Fig. 9, because it was discontinued after five days. It performed similarly to CAA in the northern hemisphere (Fig. 9a and 9b) but was very poor in the southern hemisphere (Fig. 9c and 9d). This clearly shows that the covariance structure for temperature implied by the wind/height-based statistics used in this assimilation is inappropriate for the assimilation of TOVS radiance data. The fact that BXQ is better than BYN in the northern hemisphere shows that it is important to use the correct structures for wind where conventional data dominate the analysis.

5.3 T106 forecast results

The experiment with non-separable structure functions was repeated at spectral resolution T106 (CDN, solid line) and compared with a T106 control (CAQ, dashed). The scores are shown in Fig. 10a to 10d, and they confirm the T63 results. 3D-Var with non-separable structure functions performs well in both hemispheres.

5.4 Temperature increments

The largest impact of the new structure functions is expected in the analysis increments of temperature. We saw in section 3 that the sharp vertical temperature correlations of the wind-based statistics produced large oscillations in the vertical profiles of temperature analysis increments, in analyses of some of the broad TOVS channels. Maps of model level 15 (approximately 850 hPa) temperature increments over the southern oceans, where TOVS data dominate, show very large amplitude (Fig. 11a, from experiment BXQ), far in excess of the corresponding increments produced by OI/1D-Var (Fig. 11b, BXW). The new formulation (Fig. 11c, CAA) shows a much better correspondence with the OI/1D-Var result.

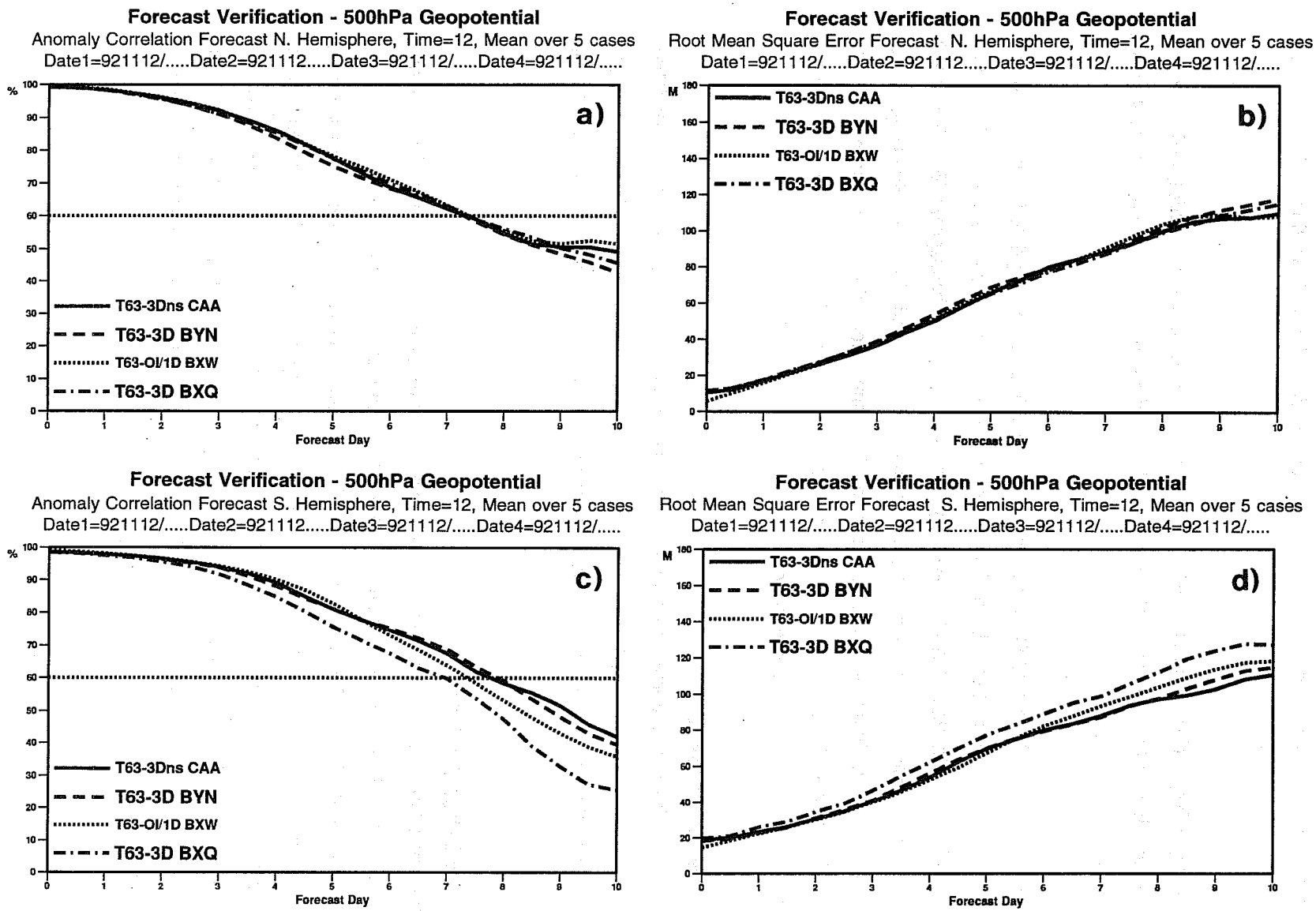

Fig.9 Like Fig.8 but averaged over 5 cases, 1992112 to 19921116 12 UT, including the experiment BXQ (dash-dotted).

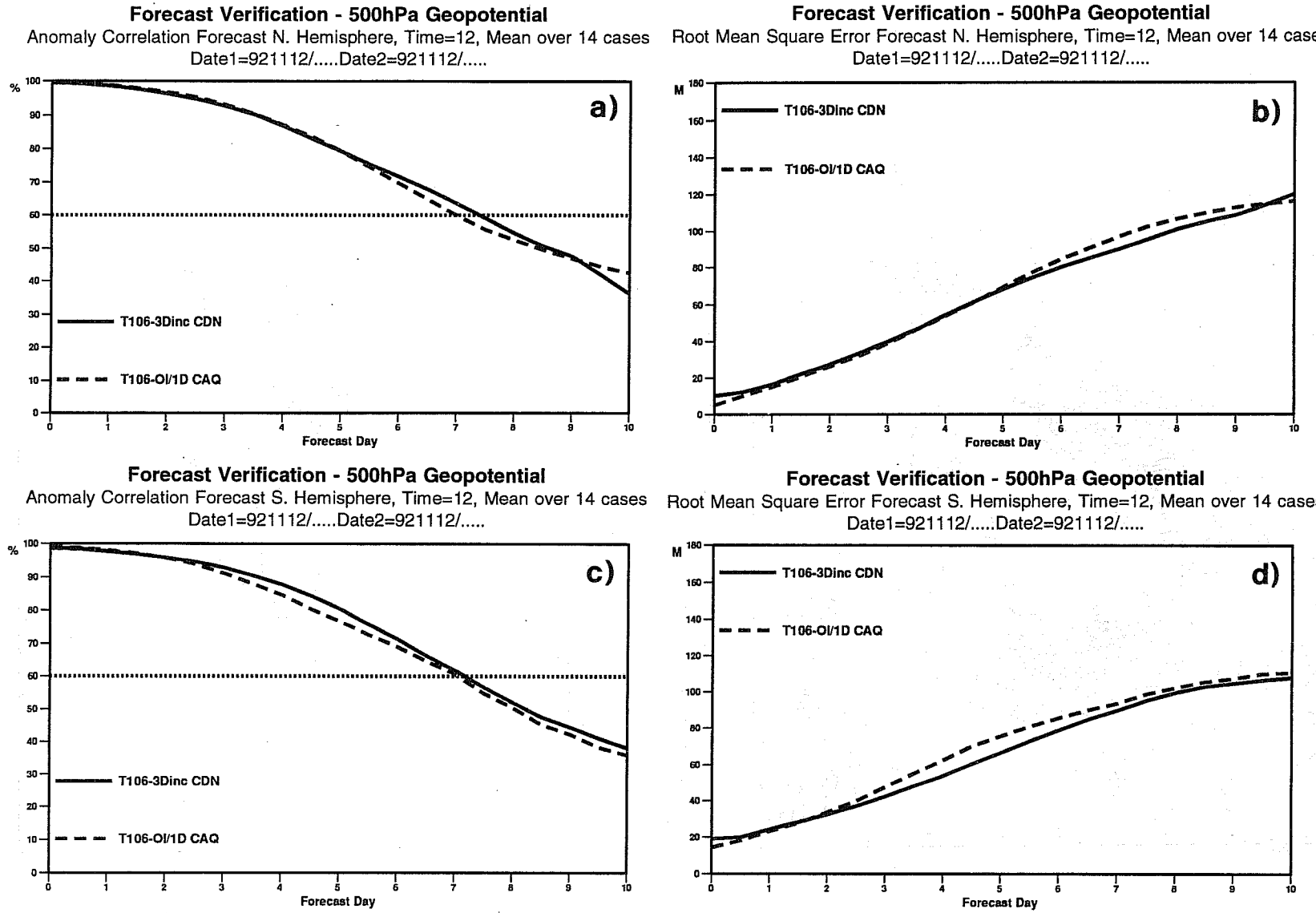

Fig.10 Like Fig.8 but for the two T106/L19 experiments: CDN, non-separable 3D-Var (full line) and CAQ, OI/1D-Var (dashed line).

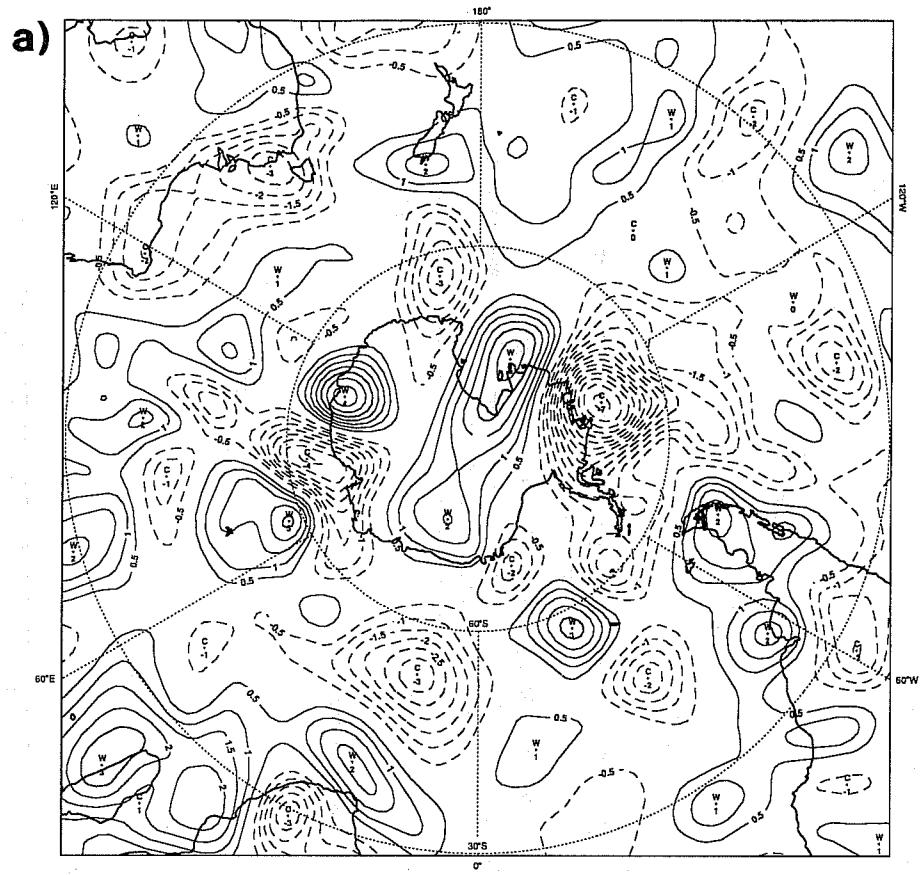

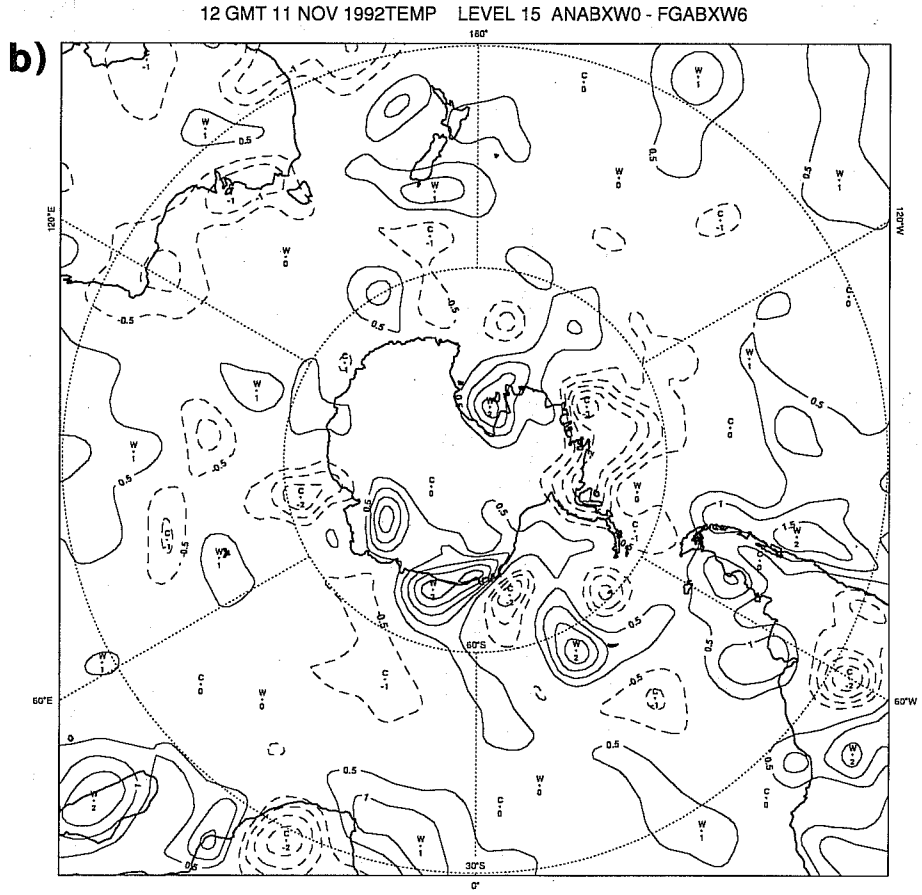

Fig.11a) Level 15 (850 hPa) analysis increments of temperature, for experiment BXQ (3D-Var, separable correct for wind). The contour interval is 0.5 K, negative dashed.

Fig.11b) Level 15 (850 hPa) analysis increments of temperature, for BXW (OI/1D-Var). The contour interval is 0.5 K, negative dashed.

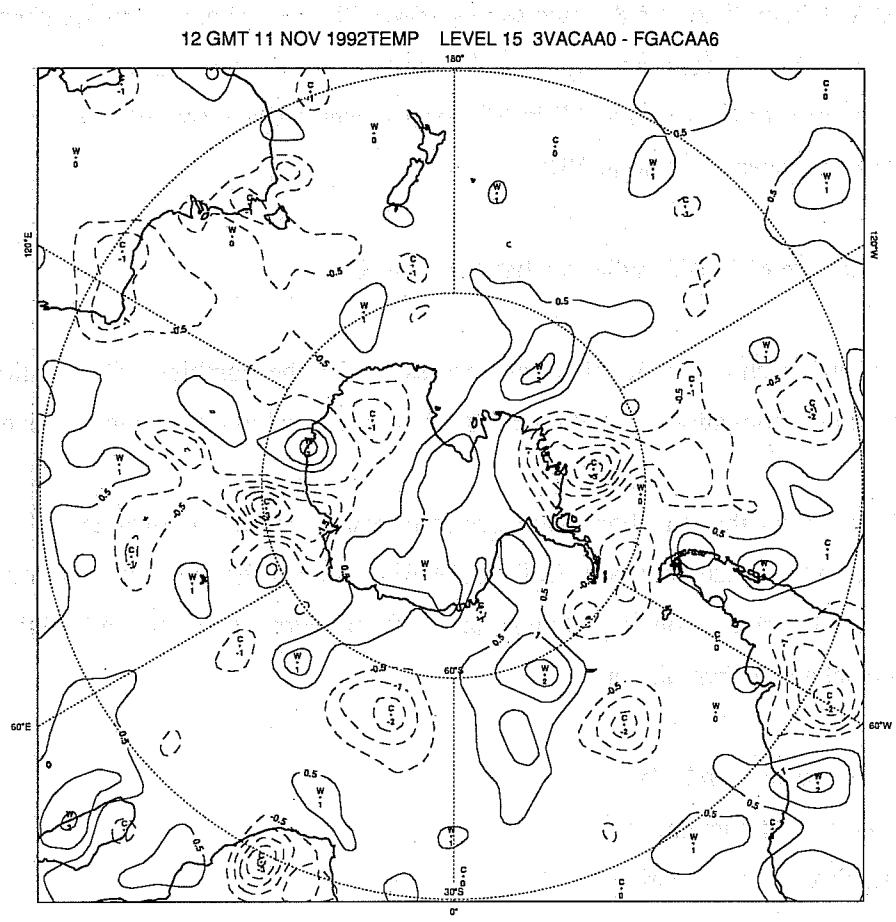

Fig.11c) Level 15 (850 hPa) analysis increments of temperature, for CAA (non-separable 3D-Var). The contour interval is 0.5 K, negative dashed.

7. CONCLUSION

These experiments have demonstrated three important points about 3D-Var:

1) The forecast scores from the 3D-Var assimilation are of a quality similar to those from the OI/1D-Var assimilation (in this two week period). 3D-Var is better in the southern hemisphere throughout the ten days, and equal in the northern hemisphere up to day four. The 3D-Var scores at T63 for days 5, 6 and 7 in the northern hemisphere are slightly worse than OI/1D-Var, but the reverse is true at T106.

2) The direct use of TOVS radiances has been successful.

3) Non-separable structure functions are necessary for the combined assimilation of 'broad' temperature information (TOVS radiances) and 'sharp' wind information (conventional data).

Non-separability means that the horizontal spectrum varies in the vertical and that the vertical correlation varies with horizontal scale. Phillips (1986) explained the effects on temperature, of non-separability. For temperature, compared to a separable formulation based on wind/height statistics, we obtain in a non-separable formulation:

i) Broader vertical correlation
ii) Shorter horizontal length-scale
iii) Smaller forecast error variance

Having introduced non-separability in 3D-Var, we now have better prospects of using temperature observations effectively. It would be interesting, for example, to experiment with using radiosonde temperature observations in this new context.

Although not yet demonstrated, we can expect the non-separable analysis to work in the following way:

A dense patch of AIREPs in the North Atlantic brings information on the small horizontal scales at the jet level. This information will be given limited vertical spread by the non-separable analysis.

The sparse surface observations in the southern hemisphere oceans measure well the large scale component of the surface pressure field. This information will be spread through a thick

layer of the atmosphere (i.e. more barotropic).

An isolated radiosonde report brings information on sharp vertical structures. This component will be given limited horizontal spread by the analysis.

TOVS data can only observe broad structures in the vertical. The non-separable analysis of these data will then mostly affect the large horizontal scales.

Acknowledgements

The authors wish to thank the members of the IFS/Arpège team at Météo-France and at ECMWF, especially P. Undén and M. Hamrud. We are also very grateful to INRIA (Institut National de Recherche en Informatique et en Automatique), Le Chesnay, France, for providing the minimisation algorithm (M1QN3).

References

Andersson, E., J. Pailleux, J-N. Thépaut, J.R. Eyre, A.P. McNally, G.A. Kelly and P. Courtier, 1994: Use of cloud-cleared radiances in three/four dimensional variational data assimilation, To appear in *Q.J.R. Meteorol. Soc.*, April-94. Also in Proc. ECMWF Workshop on "Variational Assimilation, with Special Emphasis on Three-Dimensional Aspects", Reading, 9-12 November 1992, 123-156.

Courtier, P., E. Andersson, W. Heckley, G. Kelly, J. Pailleux, F. Rabier, J-N. Thépaut, P. Undén, D. Vasiljevic, C. Cardinali, J. Eyre, M. Hamrud, J. Haseler, A. Hollingsworth, A. McNally and A. Stoffelen, 1993: Variational assimilation at ECMWF. ECMWF Tech. Memo. 194, pp 84.

Daley, R., 1991: Atmospheric data analysis, Cambridge University Press, Cambridge, pp 457.

Eyre, J.R., 1989: Inversion of cloudy satellite sounding radinaces by nonlinear optimal estimation. *Q.J.R. Meteorol. Soc.*, **115**, 1001-1037.

Eyre, J.R., G.A. Kelly, A.P. McNally, E. Andersson and A. Persson, 1993: Assimilation of TOVS radiance information through one-dimensional variational analysis. *Q.J.R. Meteorol. Soc.*, **119**, 1427-1463.

Gauthier, P., P. Courtier and P. Moll, 1993: Assimilation of simulated wind lidar data with a Kalman filter. *Mon. Wea. Rev.*, **121**, 1803-1820.

Hollingsworth, A. and P. Lönnberg, 1986: The statistical structure of short-range forecast errors as determined from radiosonde data. Part I: The wind field. *Tellus*, **38A**, 111-136.

Le Dimet, F.X. and O. Talagrand, 1986: Variational algorithms for analysis and assimilation of meteorological observations: theoretical aspects. *Tellus*, **38A**, 97-110.

Lorenc, A.C., 1986: Analysis methods for numerical weather prediction. *Q. J. R. Meteorol. Soc.*, **112**, 1177-1194.

Lönnberg, P. and A. Hollingsworth, 1986: The statistical structure of short-range forecast errors as determined from radiosonde data. Part II: The covariance of height and wind errors. *Tellus*, **38A**, 137-161.

Lönnberg, P., 1989: Quality control and filtering of satellite data. Proc. ECMWF/EUMETSAT Workshop on "Use of Satellite Data in Operational Numerical Weather Prediction: 1989-1993". Reading, 8-12 May 1989, Vol. 1, 61-80.

Pailleux, J., W. Heckley, D. Vasiljevic, J-N. Thépaut, F. Rabier, C. Cardinali and E. Andersson, 1991: Development of a variational assimilation system. ECMWF Tech. Memo. 179, pp 51.

Parrish, D.I. and J.C. Derber, 1992: The National Meteorological Centre's spectral statistical interpolation analysis system. *Mon. Wea. Rev.*, **120**, 1747-1763.

Phillips, N.A., 1986: The spatial statistics of random geostrophic modes and first-guess errors. *Tellus*, **38A**, 314-332.

Rabier, F. and T. McNally, 1993: Evaluation of forecast error covariance matrix. ECMWF Tech. Memo. 194, pp 36.

Rodgers, C.D., 1976: Retrieval of atmospheric temperature and composition from remote measurements of thermal radiation. *Rev. Geoph. Space. Phys.*, **14**, 609-624.

Smith, W.L., H.M. Woolf, C.M. Hayden, D.Q. Wark and L.M. McMillin, 1979: The TIROS-N operational vertical sounder. *Bull. Amer. Meteorol. Soc.*, **60**, 1177-1187.

Talagrand, O., 1988: Four-dimensional variational assimilation. Proc. of ECMWF Seminar on "Data Assimilation and the Use of Satellite Data", Reading, 5-9 September 1988, Vol II, 1-30.

Thépaut, J.N. and P. Moll, 1990: Variational inversion of simulated TOVS radiances using the adjoint technique. *Q. J. R. Meteorol. Soc.*, **116**, 1425-1448.

Thépaut, J.N., P. Courtier and R.N. Hoffman, 1993: Use of dynamical information in a four-dimensional variational assimilation. To appear in *Mon. Wea. Rev.* Also available in Proc. ECMWF Workshop on "Variational Assimilation with Emphasis on Three-dimensional Aspects". Reading, 9-12 November 1992, 237-269.